Copper nanoparticle selectively encapsulated with ultrathin carbon cage loaded on $SrTiO_3$ as stable photocatalyst for visible-light H_2 evolution via water splitting

Lihang Tong,[a] *Liteng Ren,*[a] *Ao Fu,*[b] *Defa Wang,*[a,b] *Lequan Liu*[*,a,b] *and Jinhua Ye*[a,b,c]

[a]TJU-NIMS International Collaboration Laboratory, Key Laboratory of Advanced Ceramics and Machining Technology (Ministry of Education) and Tianjin Key Laboratory of Composite and Functional Materials, School of Material Science and Engineering, Tianjin University, Tianjin 300072, China

[b]Collaborative Innovation Center of Chemical Science and Engineering (Tianjin), Tianjin 300072, China

[c]International Center for Materials Nanoarchitectonics (WPI-MANA) and Environmental Remediation Materials Unit, National Institute for Materials Science (NIMS), Japan

* Correspondence to: Lequan.Liu@tju.edu.cn (L. Liu).

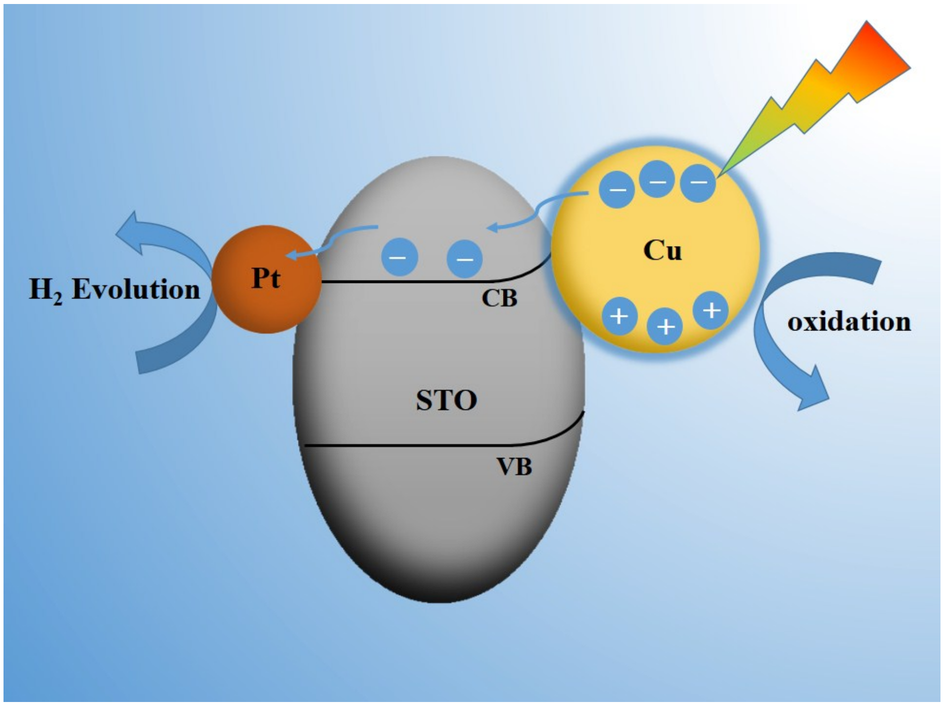

Scheme S1 A simple mechanism for the hydrogen evolution over this Cu@C/$SrTiO_3$ catalyst

In this Cu@C/STO MIP system, visible-light photons were first absorbed by Cu nanoparticles. Then, the excited hot electrons in Cu nanoparticles transfer from Cu to the CB of adjacent $SrTiO_3$ and participate in the subsequent reduction. This mechanism is similar to that of a dye-sensitized solar cell.

MATERIALS AND METHODS

Chemicals:

All chemical reagents were purchased from Sinopharm Chemical and Sigma-Aldrich. All chemical reagents were used without further purification. Distilled water was used in all experiments.

Synthesis of Cu/$SrTiO_3$:

$SrTiO_3$ was fabricated by a modified polymerize-calcine (PC) method, as we previously reported.[1] In brief, 2.88ml $Ti(OC_4H_9)_4$ was dissolved in 10 ml 2-methoxyethanol, denoted as solution A. Then, 2.18 g $SrCl_2$•$6H_2O$ was dissolved in 10 ml 2-methoxyethanol, denoted as solution B, and 30 g citric acid was dissolved in 30 ml 2-methoxyethanol with heating, denoted as solution C. Solutions A and B were mixed and stirred for 0.5 h to obtain a sol. This sol was transmitted to solution C and continually stirred for 10 min. After that, 5 ml dehydrated ethylene glycol was added. The mixture was then heated to 125 ℃ at an increasing rate of 1 ℃ min^{-1} and maintained for 20 h to evaporate the 2-methoxyethanol solvent. Subsequently, polymerization was carried out at 130 ℃ for another 20 h. The obtained brown resin was cooled to room temperature. Finally, the resin was heated in a stove at 300 ℃ for 3 h and calcined at 500 ℃ for 5 h at an increasing rate of 1 ℃ min^{-1}. The resulting white powder was denoted as STO.

Cu/STO photocatalysts with different weight percentage of Cu loadings (2-4 %) were prepared with chemical reduction method. Typically, 0.0453 g copper nitrate ($Cu(NO_3)_2$•$2.5H_2O$) and 0.4 g STO were dissolved in deionized water, and stirred 30 minutes to form a light blue-green solution, denoted as solution A. Then, excess sodium borohydride ($NaBH_4$) was dissolved in deionized water, denoted as solution B. After stirring, solution B was added into solution A. The mixture was continually stirred for 1 hour, then centrifuged, washed, dried at 60 ℃ for 12h and obtained the CuO/STO system. Finally, the CuO/STO system was reduced at 600 ℃ for 3 hours at a gas flow of 100 sccm mixed gases of Ar and H_2 (VAr: VH_2=9:1) to obtained the Cu/STO system. The proportion of Cu in Cu/STO was adjusted by varying the weight ratio of Cu.

Synthesis of Cu@C/STO:

The Cu@C/STO photocatalysts was fabricated by a chemical vapor deposition (CVD) method. Ethyne gas was used as carbon source. First, the pristine CuO/STO was heated to 600 ℃ at an increasing rate of 10 ℃ min^{-1} and maintained for 2.5 hours at a gas flow of 100 sccm mixed gases of Ar and H_2 (VAr:VH_2=9:1). Finally, 5 sccm ethyne (C_2H_2) was introduced in the chamber. After the graphene growth, the C_2H_2 gas flow was shut down, and the sample was cooled down to room temperature under H_2 and Ar gas. The Cu@C/STO with different thickness of carbon cages were obtained by adjusting the time of graphene growth for 2 min, 4 min and 6 min. For each sample, the total volume of ethyne being used is 10 ml, 20 ml and 30 ml, respectively. So, the catalysts were labeled as Cu@C/STO-yml (y=10, 20, 30).

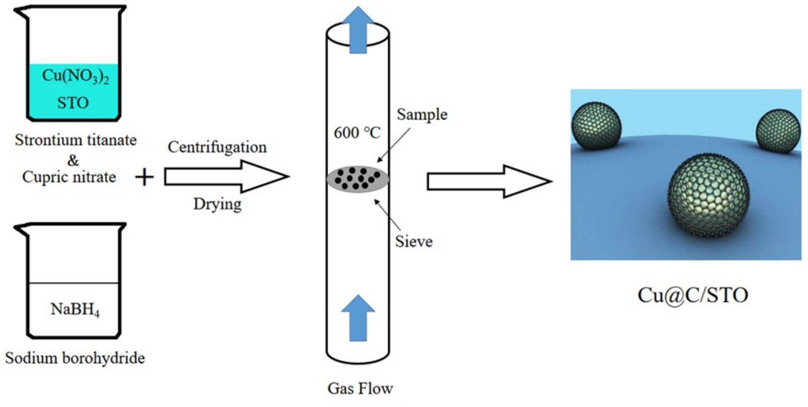

Scheme S2 Schematic illustration for the preparation process of Cu@C/STO.

Characterizations:

The XRD patterns were obtained with a powder X-ray diffractmeter (Cu Kα radiation, D8 Advanced, Bruker, Germany). The morphology of the sample was observed with transmission electron microscopy (TEM, Tecnai G2 F20, FEI, USA). The absorption spectra were converted from the UV−visible diffuse reflectance spectra measured on a UV−visible spectrophotometer (UV-3600, Shimadzu, Japan). Raman analysis was recorded on a Raman microscope (Raman, HORIBA Scientific, Japan). Chemical valence analysis was performed by X-ray photoelectron spectroscopy (Escalab 250Xi, Thermo Scientific, America).

Photocatalytic Activity Evaluation:

The measurement of photocatalytic H_2 evolution was carried out in a glass reactor connected with a closed gas circulation system. The light source was a 300 W Xe arc lamp. The photocatalyst of Cu@C/STO (100 mg) was dispersed in aqueous methanol (50 mL of methanol and 220 mL of H_2O) with a magnetic stirrer. The cocatalyst Pt (0.5 wt %) was loaded via an in situ photodeposition method (λ >300 nm). The Pt precursor was an aqueous solution of H_2PtCl_6. The photocatalytic H_2 evolution was tested under visible-light irradiation (equipped with an L42 cutoff filter, λ >400 nm). The evolved H_2 was detected by an online gas chromatograph (GC-2014 with TCD, Shimadzu, Japan).

Photocatalytic O_2 evolution was carried out with 0.1 g of photocatalyst suspended in 270 ml water in the presence of 5 mmol $AgNO_3$ as a sacrifice reagent. A 300 W Xe arc lamp was employed as the light source. For visible-light (λ >400 nm) reaction, a L42 cutoff filter was used to remove UV light. The concentrations of O_2 were detected by a gas chromatograph (GC-8A with TCD, Shimadzu).

Catalytic Reduction of 4-NP to 4-AP:

This reaction was performed under atmosphere environment, and all of the catalyst was stored in air for 1 month. So, the reduction of 4-NP by $NaBH_4$ was chosen to test the stability and catalytic efficiency of the Cu@C/STO. Typically, aqueous solutions of 4-NP (0.125 mM, 3 ml) and freshly aqueous solutions of $NaBH_4$ (1.0 M, 0.3 ml) were added to a quartz cuvette and became a bright yellow solution. Then 0.2 ml, 0.2 mg ml^{-1} aqueous solution of catalysts was added into the bright yellow solution. This reaction was in-suit monitored by UV-vis absorption measurement.

SUPPLEMENTARY FIGURES

Table S1. H_2 evolution over different photocatalyst under visible light irradiation.

Photocatalysts	Cocatalyst	Sacrificial reagents	Catalyst Amount (mg)	H_2 evolution rate (μmol h^{-1})	Ref.
Cu@C/STO	Pt	Methanol	100	≈11	This work
Cu/P25-graphene	Pt	Methanol	20	≈8	2
CuAu alloy/STO	Pt	Methanol	200	≈6	3
Carbon Nitride (CN)	Pt	Triethanolamine (TEOA)	50	≈7.9	4
CN/CdS	Pt	Ethanol	100	17.27	5
$Zn_{0.2}Cd_{0.8}S$	-	0.35 M Na_2S/0.25 M Na_2SO_3	50	≈12.3	6
SiO_2-Au-Ta_2O_5	Pt	Methanol	50	≈4	7
CdS/$ZnWO_4$	-	0.35 M Na_2S/0.25 M Na_2SO_3	100	≈4	8
AgInZnS/MoS_2	-	Lactic acid	50	≈20	9
Ag/AgI/CN	-	TEOA	70	≈5	10
TaON@Ta2O5	Rh	Methanol	200	≈9	11

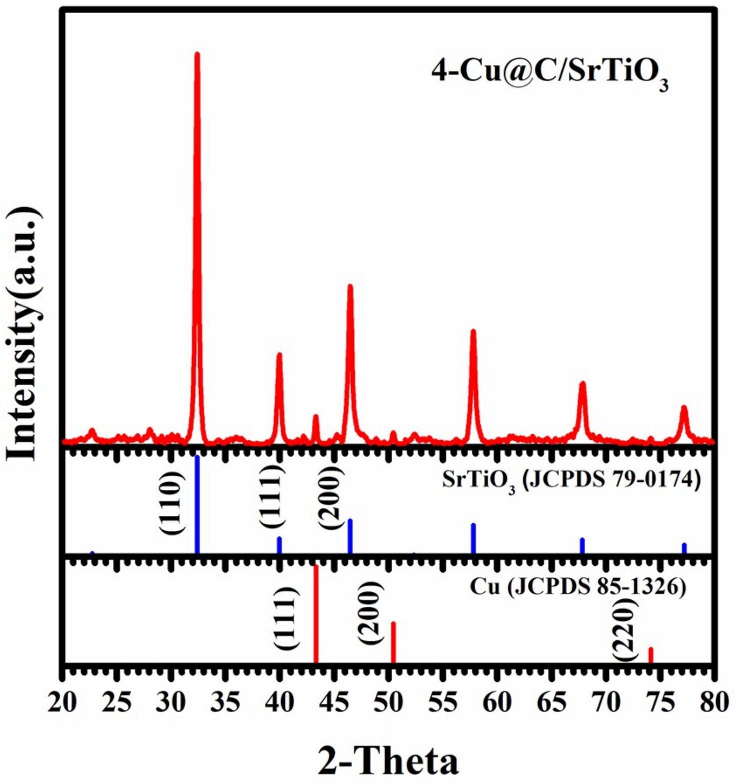

Fig. S1 XRD pattern of 4 wt% Cu@C/STO.

Table S2. Theoretical and actual Cu weight ratios of catalysts.

Catalysts	Theoretical Cu Loading (wt%)	Actual Cu Loading (wt%)	Actual Cu weight in reaction (mg)	Normalized H_2 rate (mmol g^{-1} h^{-1})
Cu@C/STO	2	1.80	1.8	25.88
Cu@C/STO	3	2.47	2.47	41.30
Cu@C/STO	4	3.51	3.51	21.35

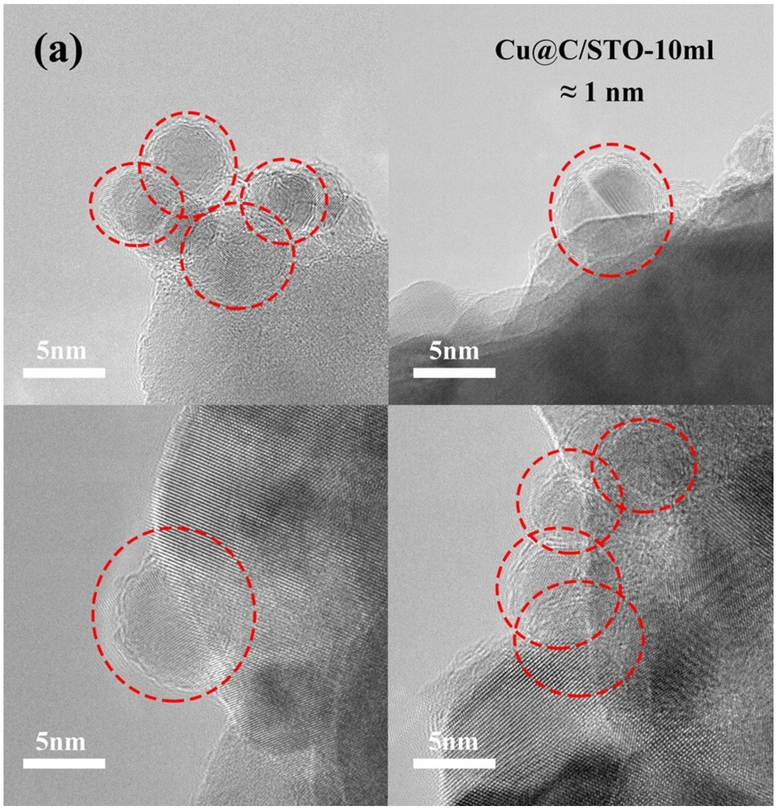
(a)
Cu@C/STO-10ml
≈ 1 nm
5nm
5nm
5nm
5nm

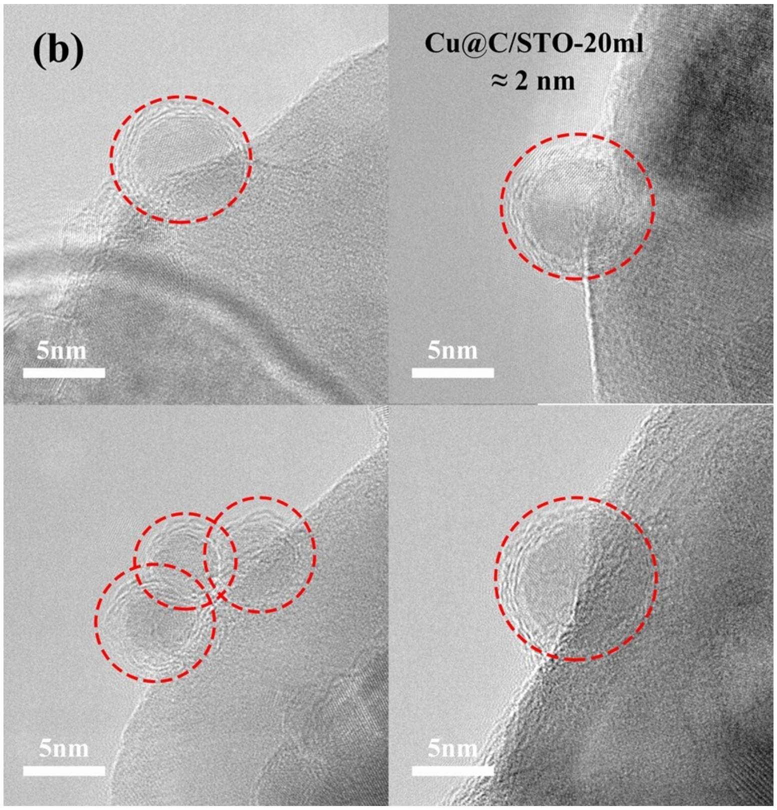
(b)
Cu@C/STO-20ml
≈ 2 nm
5nm
5nm
5nm
5nm

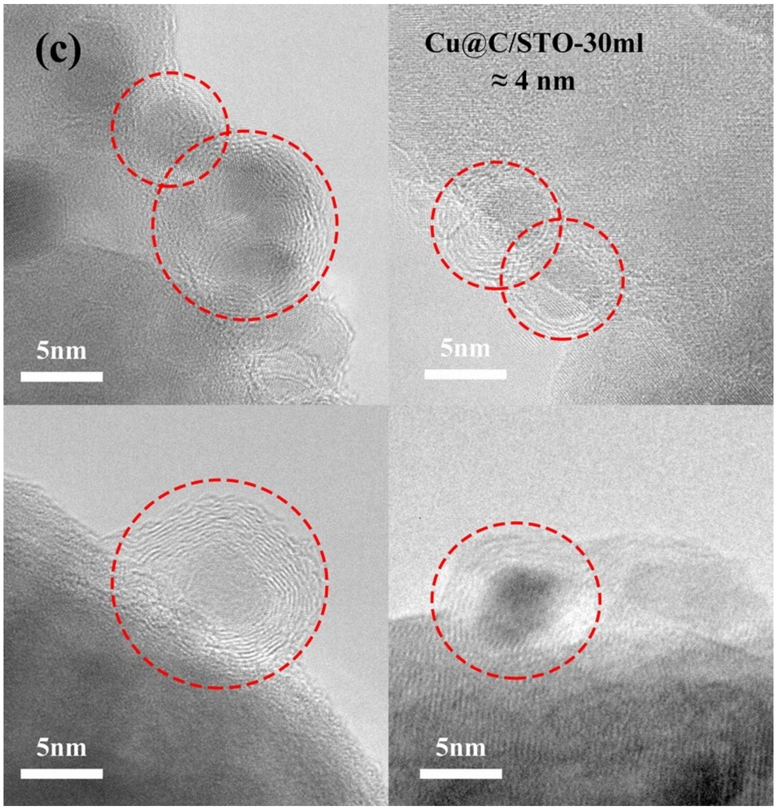

Fig. S2 HRTEM images of (a) Cu@C/STO-10ml, (b) Cu@C/STO-20ml and (c) Cu@C/STO-30ml.

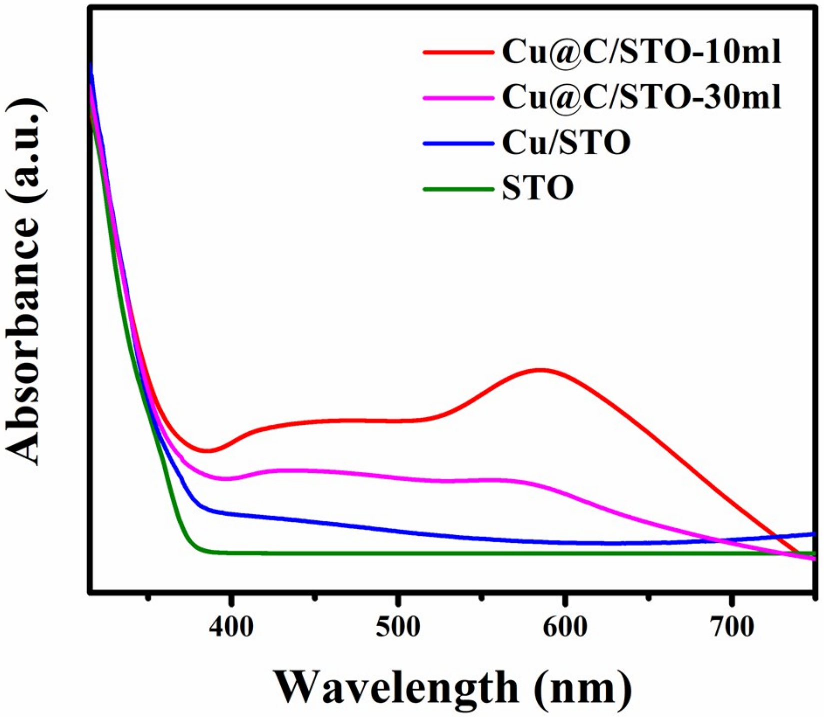

Fig. S3 UV-Vis absorption spectrum of pristine STO, Cu/STO and Cu@C/STO with different volume of ethyne used in CVD reaction, the weight percentage of Cu loading is 3 wt%.

Table S3. H_2 evolution over Cu/STO samples with different chemical compositions.

Catalysts	Metal Loading (wt%)	H_2 Evolution (μmol g^{-1} h^{-1})
Cu/STO	2	47.2
Cu@C/STO	2	46.0
Cu/STO	3	103.2
Cu@C/STO	3	102.3
Cu/STO	4	75.6
Cu@C/STO	4	74.5

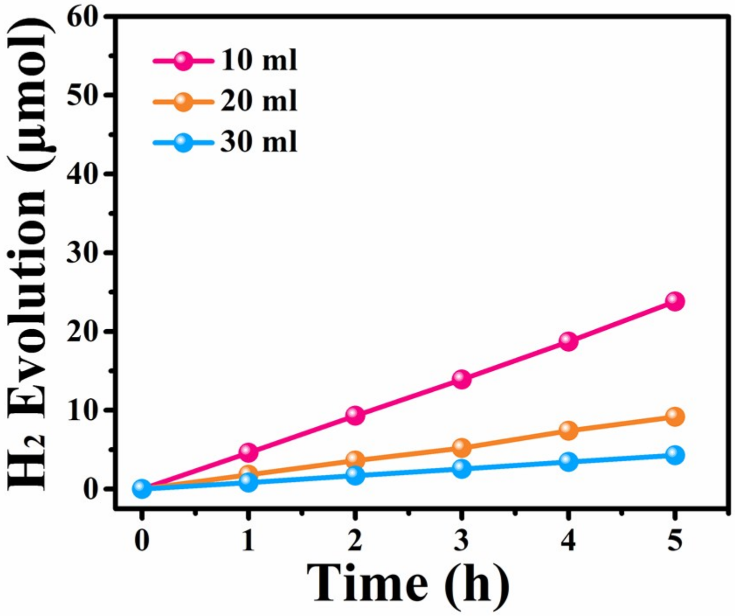

Fig. S4 Curve of H_2 evolution as a function of irradiation time over 2 wt% Cu@C/STO with different thickness of carbon cages.

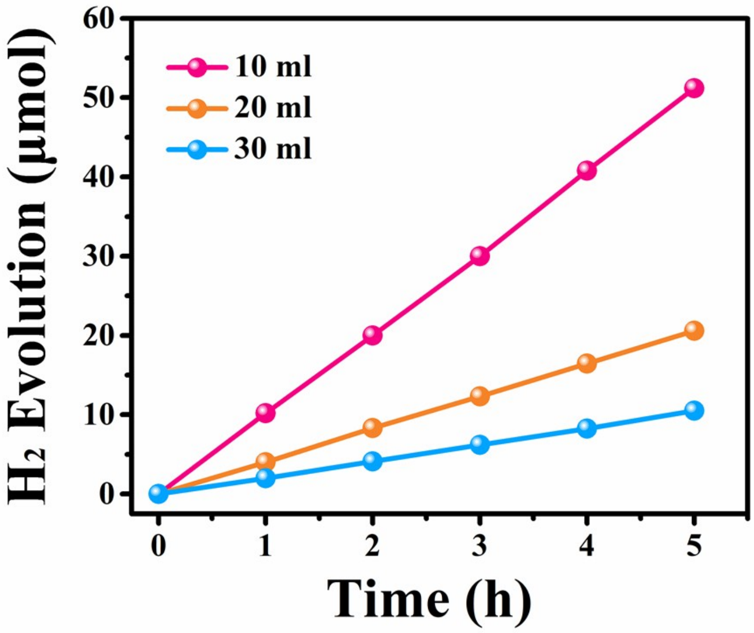

Fig. S5 Curve of H_2 evolution as a function of irradiation time over 3 wt% Cu@C/STO with different thickness of carbon cages.

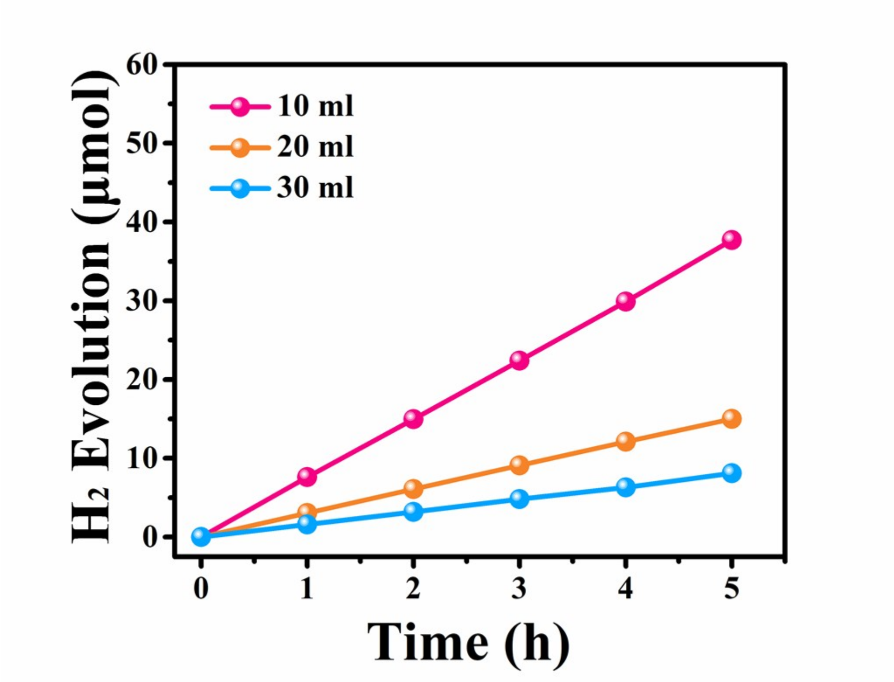

Fig. S6 Curve of H_2 evolution as a function of irradiation time over 4 wt% Cu@C/STO with different thickness of carbon cages.

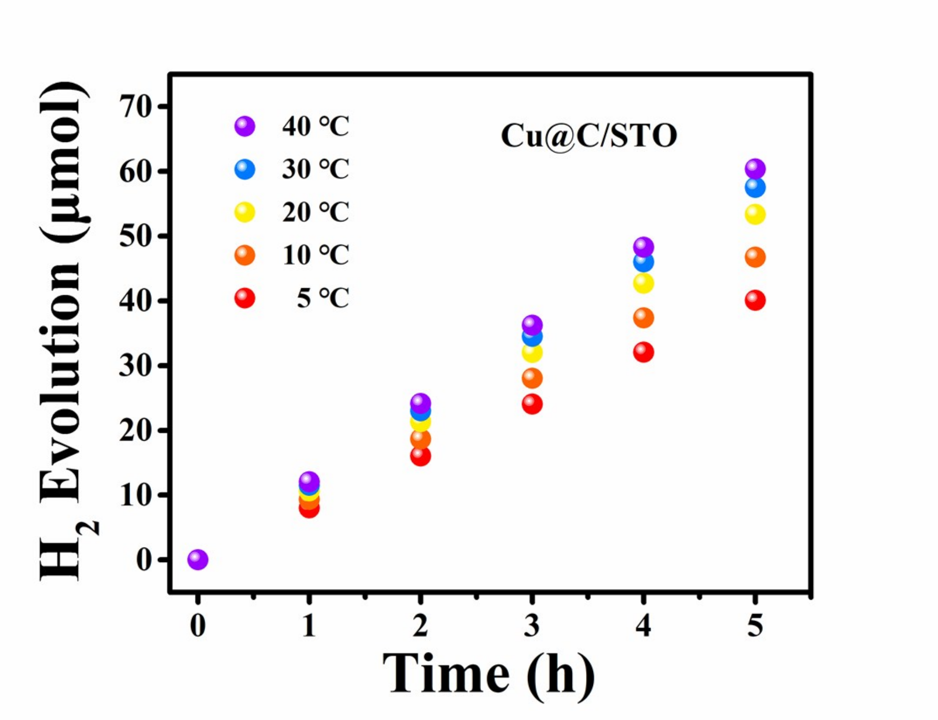

Fig. S7 Reaction kinetics test for 3 wt% Cu@C/STO-10ml under different reaction temperatures. Reaction conditions: 0.1 g catalyst, under visible light (300 W Xe lamp with L42 filter, λ > 400 nm).

To further elucidate the influence of temperature, a reaction kinetics test was conducted and the results were concluded in the following figure. As can be seen, the hydrogen evolution rate gets higher when the reaction temperature is raised. This is because the photocatalytic hydrogen evolution via water splitting reaction includes surface reaction which is a thermocatalytic reaction and greatly influenced by temperature. Besides, from this figure, the reaction rate growth is slowing as the temperature becomes higher. This is because the maximum rate is decided by the number of generated electrons.

Moreover, the hydrogen evolution rate with controlled temperature at 30 ℃ is closest to the activity which is achieved in Fig. 2. This is an expected result because the room temperature is around 20 ℃ when this reaction was conducted and the 300 W Xe lamp will slightly heat the water. Considering that the 300 W Xe lamp is a common light source in evaluating the activity of photocatalysts, the reaction activity in main text is reliable and comparable.

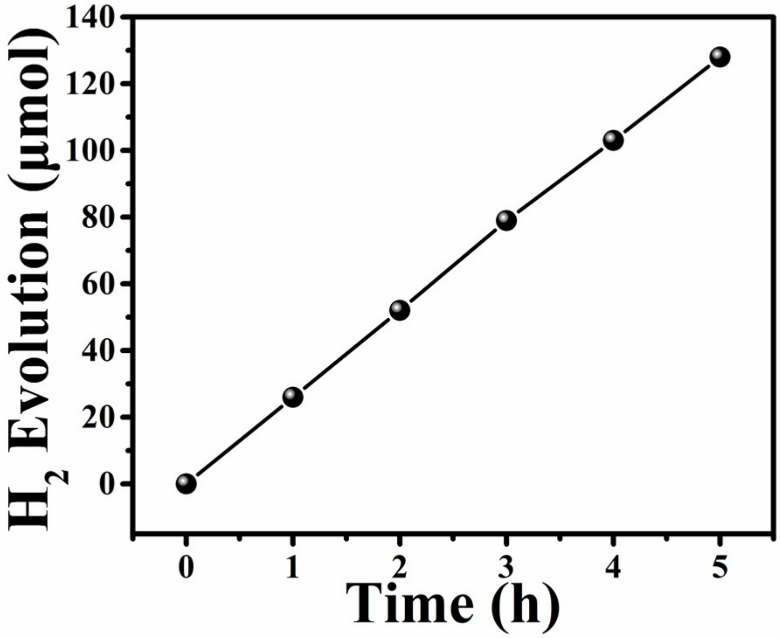

Fig. S8 H_2 evolution of 3 wt% Cu@C/STO-10ml with ascorbic acid as the sacrificial agent. Reaction conditions: 0.1 g catalyst, under visible light (300 W Xe lamp with L42 filter, λ > 400 nm).

Since both of the half reactions of water splitting were conducted, the overall water splitting reaction was also performed using Cu@C/STO-10ml catalyst. After photodepositing Pt cocatalyst, the sample was centrifuged and washed. Then the overall water splitting reaction was conducted. The results are shown in the following figure.

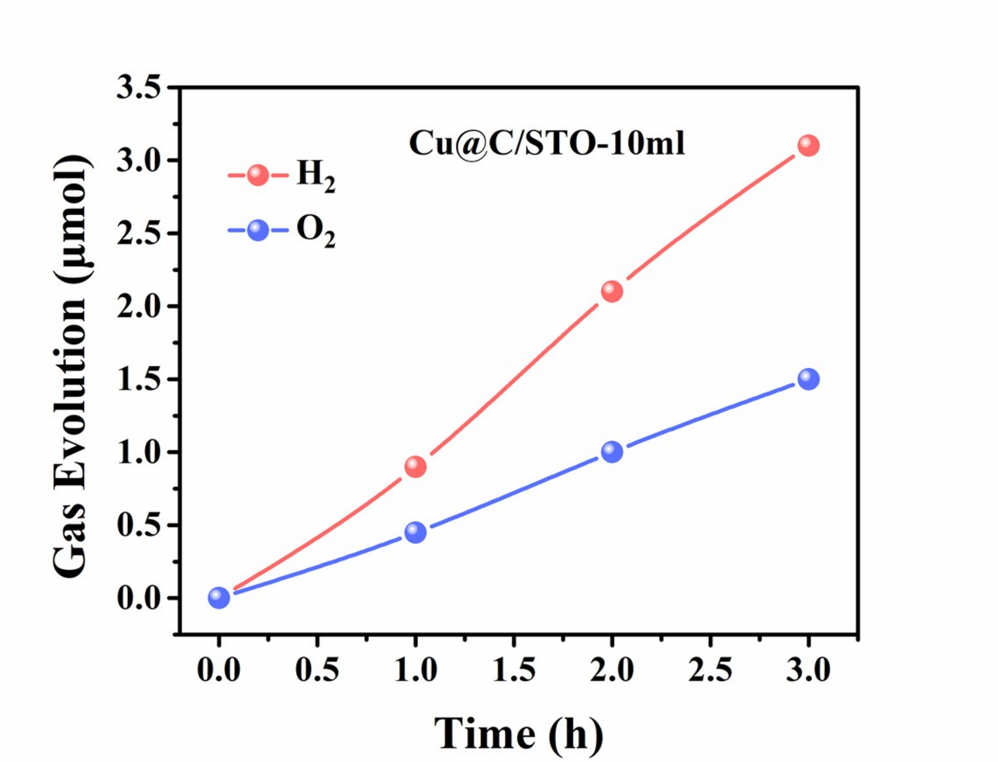

Fig. S9 Photocatalytic overall water splitting reactivity for Cu@C/STO-10ml. (Reaction conditions: photocatalyst, 0.2 g; reaction solution, 270 mL distilled water; light source, 300 W Xe lamp with L42 cutoff filter, λ >400 nm.)

As can be seen, Cu@C/STO-10ml catalyst gives stoichiometric H_2 and O_2 evolution from pure water though the evolution rate is relatively low at the present stage. Taking account of the fact that overall water splitting was driven only by Cu absorbing visible photons and the weight percentage of Cu accounts for only 3%, there are still many challenges to be addressed in the future study. For example, the H_2 and O_2 backward reaction takes place on the surface of cocatalyst, thereby hindering the forward reaction.

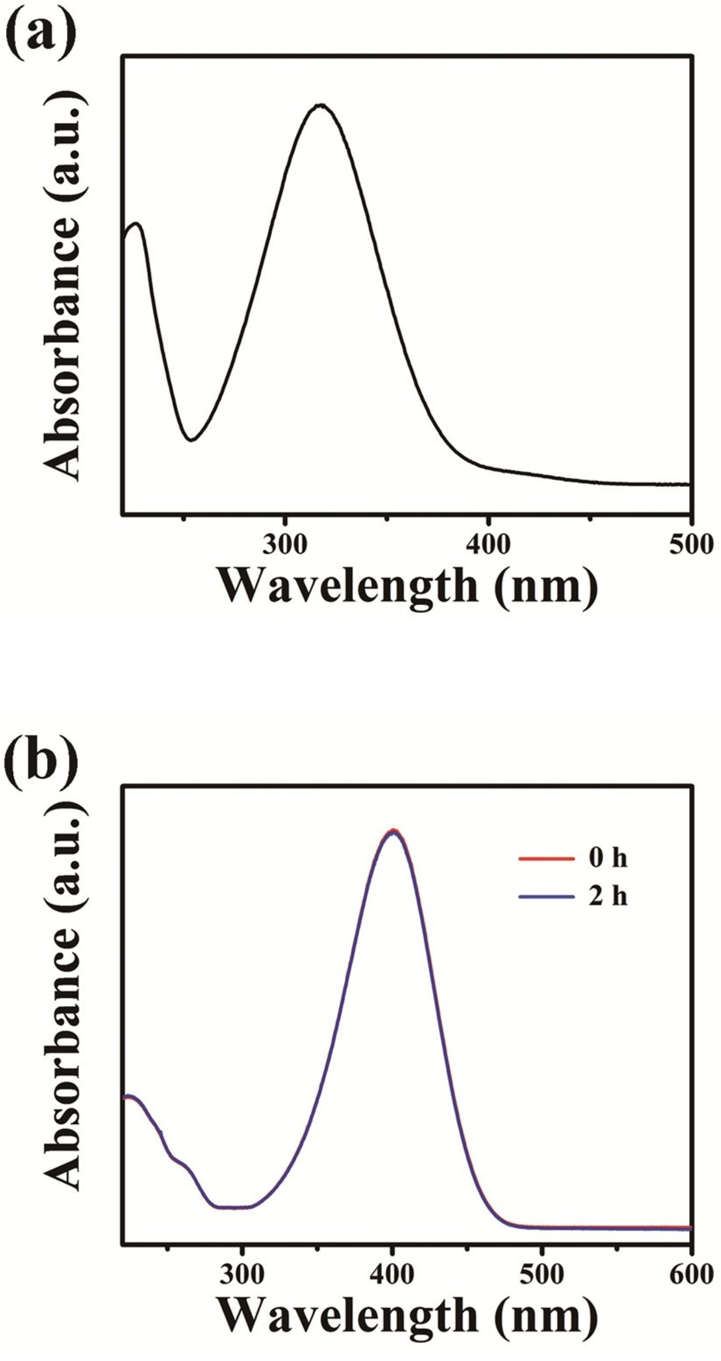

Fig. S10 (a) UV-vis spectrum of 4-NP in aqueous solution. (b) UV-vis spectra for the 4-NP reduction by $NaBH_4$ at 25 °C with STO.

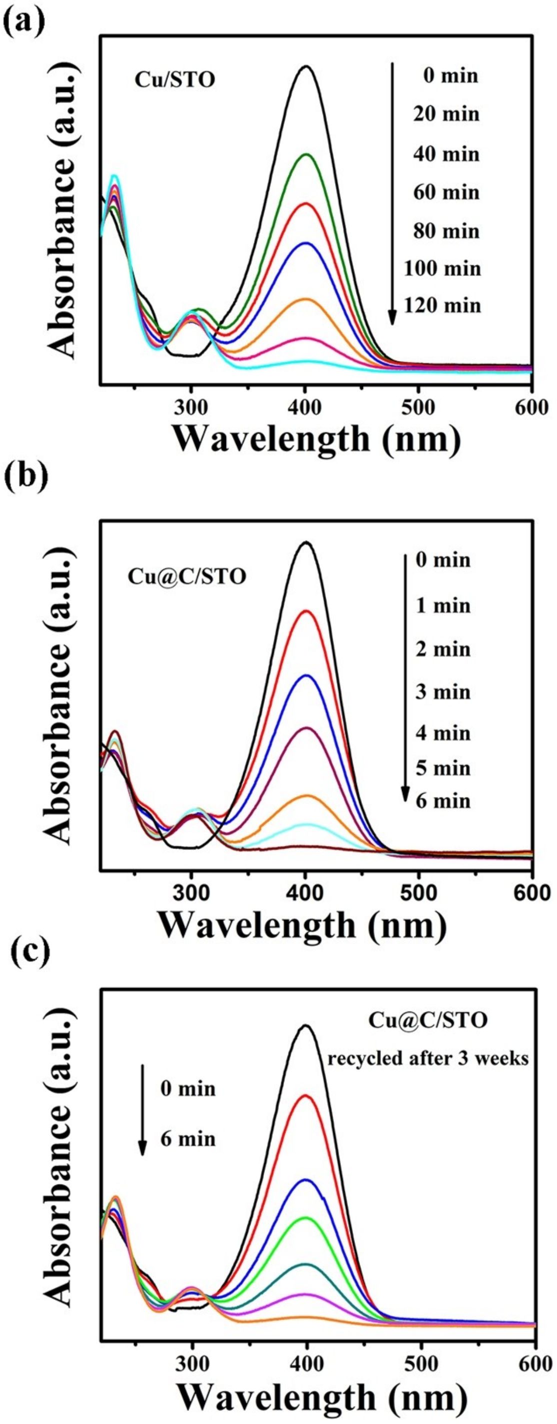

Fig. S11 UV-vis spectra for the 4-NP reduction by $NaBH_4$ at 25 °C with (a) Cu /STO, (b) Cu@C/STO and (c) Cu@C/STO recycled after 3 weeks, respectively.

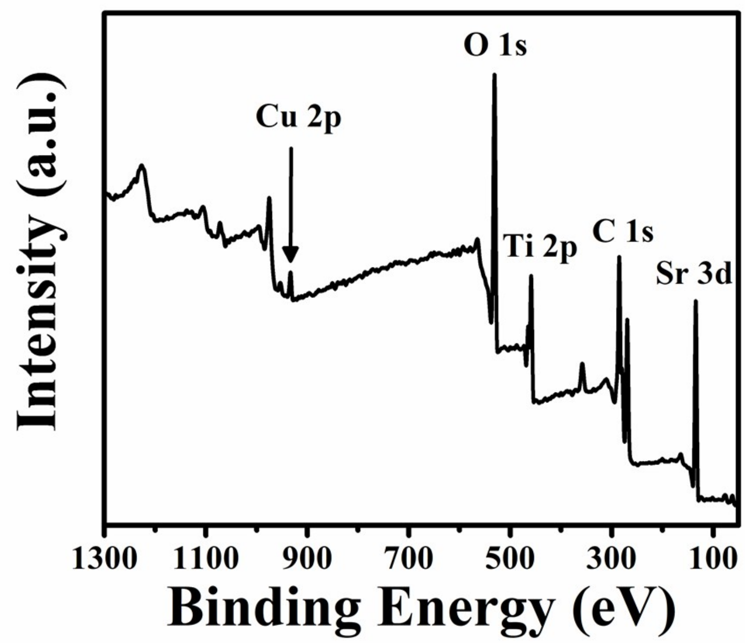

Fig. S12 XPS survey spectrum for Cu@C/STO catalysts.

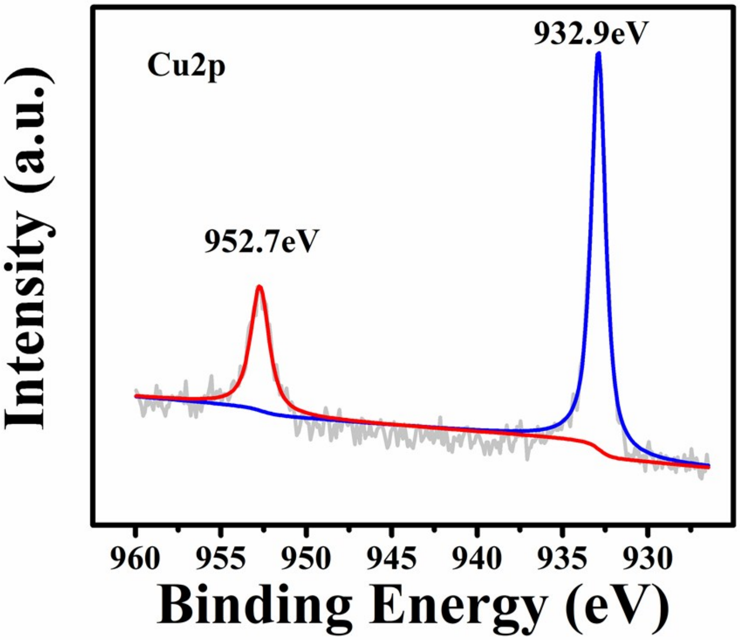

Fig. S13 Detailed Cu 2p XPS spectrum for Cu@C/STO catalysts after water splitting reaction.

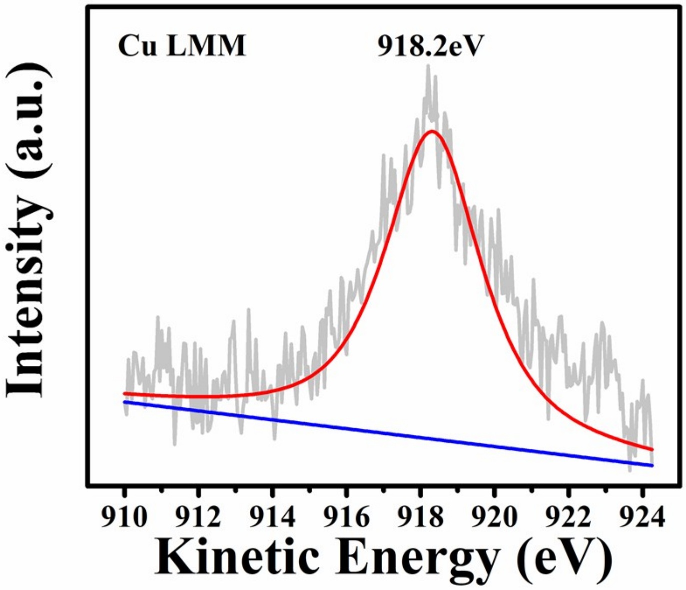

Fig. S14 Detailed Cu LMM spectrum for Cu@C/STO catalysts after water splitting reaction.

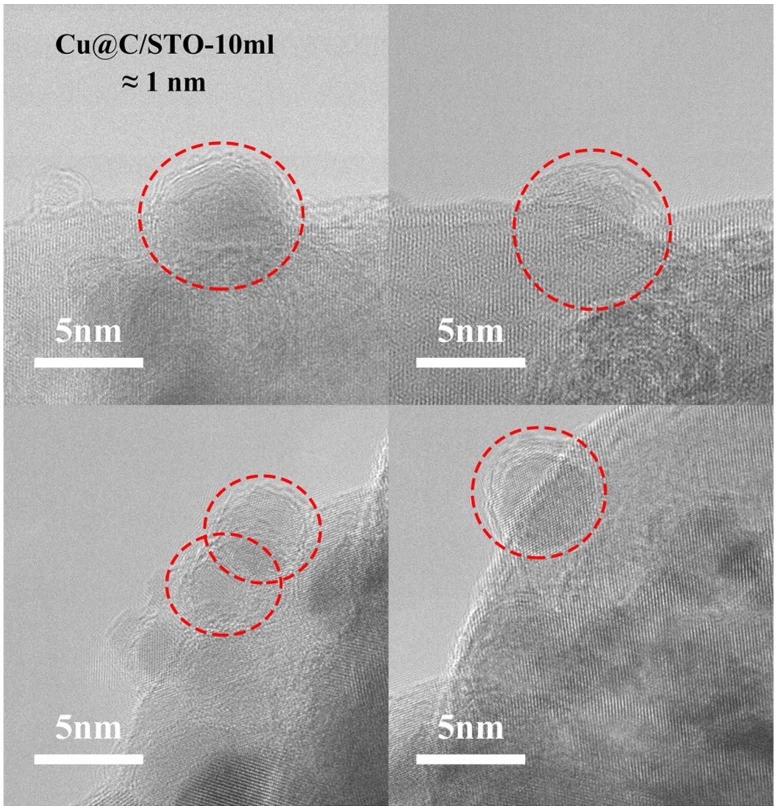

Fig. S15 HRTEM images of Cu@C/STO-10ml catalysts after water splitting reaction.

References

[1] L. Q. Liu, P. Li, B. Adisak, S. X. Ouyang, N. Umezawa, J. H. Ye, R. Kodiyath, T. Tanabe, G. V. Ramesh, S. Ueda, H. Abe, *J. Mater. Chem. A* 2014, **2**, 9875-9882.

[2] X.-J. Lv, S.-X. Zhou, C. Zhang, H.-X. Chang, Y. Chen and W.-F. Fu, *J. Mater. Chem.*, 2012, **22**.

[3] M. Liu, W. Zhou, T. Wang, D. Wang, L. Liu and J. Ye, *Chem. Commun.* 2016, **52**, 4694-4697.

[4] Y. Kang, Y. Yang, L. C. Yin, X. Kang, G. Liu and H. M. Cheng, *Adv. Mater.* 2015, **27**, 4572-4577.

[5] L. Ge, F. Zuo, J. Liu, Q. Ma, C. Wang, D. Sun, L. Bartels and P. Feng, *J. Phys. Chem. C* 2012, **116**, 13708-13714.

[6] L. Yin, F. Zhang, L. Feng, J. Huang, X. Kong, H. Zhang, H. Li and X. Wang, *Int. J. Hydrogen Energy* 2019, **44**, 23868-23879.

[7] X. Liu, J. Feng, B. Wu, Y. Li, W. Xie, J. Lin, X. Zheng, X. Luo and A. A. Al Kheraif, *Int. J. Hydrogen Energy* 2018, **43**, 20546-20562.

[8] N. Zhang, D. Chen, B. Cai, S. Wang, F. Niu, L. Qin and Y. Huang, *Int. J. Hydrogen Energy* 2017, **42**, 1962-1969.

[9] T. Huang, W. Chen, T.-Y. Liu, Q.-L. Hao and X.-H. Liu, *Int. J. Hydrogen Energy* 2017, **42**, 12254-12261.

[10] C. Bai, J. Bi, J. Wu, Y. Xu, S. Wohlrab, Y. Han and X. Zhang, *Int. J. Hydrogen Energy* 2019, **44**, 21397-21405.

[11] H. Jiang, W. Zhang, S. Zang and W. Zhang, *Int. J. Hydrogen Energy* 2019, DOI: 10.1016/j.ijhydene.2019.07.166.